1   **An oral vaccine for SARS-CoV-2 RBD mRNA-bovine milk-derived**

2   **exosomes induces a neutralizing antibody response *in vivo***

3   Quan Zhang[1,#], Miao Wang[1,#], Chunle Han[1], Zhijun Wen[1], Xiaozhu Meng[1], Dongli

4   Qi[1], Na Wang[1], Huanqing Du[1], Jianhong Wang[1], Lu Lu[1,*], Xiaohu Ge[1,2,*]

5   [1]Tingo Exosomes Technology Co., Ltd, Tianjin, China

6   [2]Tingo Regenerative Medicine Technology Co., Ltd, Tianjin, China

7   [#] These authors contributed equally to this work.

8   *Correspondence to lulu@tingocell.com (Lu Lu) and gexiaohu@tingocell.com

9   (Xiaohu Ge)

10   **Abstract**

11   The severe acute respiratory syndrome coronavirus type 2 (SARS-CoV-2) that

12   causes the coronavirus disease 2019 (COVID-19) has presented numerous

13   challenges to global health. The vaccines, including lipid-based nanoparticle

14   mRNA, inactivated virus and recombined protein, have been used to prevent

15   SARS-CoV-2 infections in clinics and are immensely helpful against the

16   epidemic. Here, we first present an oral mRNA vaccine based on bovine

17   milk-derived exosomes (milk-exos), which encodes the SARS-CoV-2 receptor

18   binding domain (RBD) as an immunogen. The results indicated that RBD mRNA

19   delivered by milk-derived exosomes can produce secreted RBD peptide in 293

20   cells *in vitro* and stimulated neutralizing antibodies against RBD in mice. These

21   results indicated that bovine milk-derived exosome-based mRNA vaccine could

22   serve as a new strategy for preventing SARS-CoV-2 infection. Meanwhile, it also

23   can work as a new oral delivery system for mRNA.

24   **Keywords:** bovine milk-derived exosomes; SARS-CoV-2; receptor binding

25   domain; mRNA; oral vaccines; neutralizing antibody

26   **One Sentence Summary:** Oral SARS-CoV-2 mRNA vaccine based on bovine

27 milk-derived exosomes can stimulate neutralizing antibodies in mice.

28 **Introduction**

29 COVID-19 typically presents symptoms common to many respiratory infections,

30 including fever and cough. Still, in many cases, it progresses to a more severe

31 disease that may include acute respiratory distress, disseminated disease, and

32 death (1-3). The SARS-CoV-2 Spike protein is a homotrimeric transmembrane

33 glycoprotein composed of S1 and S2 subunits. When spike protein interacts with

34 specific receptors on host cells, its receptor binding domain (RBD) is located at

35 the C-terminus of S1 and can specifically bind to the receptor

36 angiotensin-converting enzyme 2 (ACE2) and initiates the membrane fusion

37 between the virus and host cell (4-7). Studies have shown that RBD is the main

38 target of most of the neutralizing activity in immune serum, suggesting that RBD

39 may be a potential target for the 2019-nCoV vaccine or therapy (8-10).

40 Currently, the available platforms for COVID-19 vaccines include inactivated

41 vaccines, live attenuated vaccines, recombinant protein vaccines, viral vector

42 vaccines, and nucleic acid vaccines (11). In 2021, the revenue of COVID-19

43 vaccine products of global key enterprises showed that Pfizer and German

44 BioNTechnology's mRNA vaccine revenues were 367.8 billion dollars and 213.6

45 billion dollars, respectively, accounting for more than half of the global vaccine

46 market share. Pfizer's mRNA vaccine accounted for the highest proportion

47 because it rapidly attracted great attention and promotion for its safety, high

48 efficiency, and short production cycles. Compared with other vaccine technology

49 platforms, the mRNA vaccine platform also has these advantages, including 1.

50 an excellent immune effect; 2. a short R&D cycle; 3. convenient large-scale

51 production (12, 13); 4. no risk of infection or genome integration (14-16); 5. the

52 human expression system expresses antigens with good immunogenic recovery

53 (17); 6 the stimulation of humoral and cellular immunity (18, 19); 7. no adjuvant,

54 and so on. However, mRNA vaccines are also flawed, with high technical

55 barriers and delivery technology patent restrictions; they are unstable and

56 inconvenient to preserve and transport. Traditionally, it needs an intramuscular

57 injection and a professional operation.

58 Most vaccines now undergoing clinical trials are injected intramuscularly or

59 subcutaneously, restricting immune activation to the few draining lymph nodes

60 (20, 21). Oral administration is thought to have a higher safety profile, better

61 patient compliance, and lower medical costs than injection (20, 22). The

62 difficulties of the complex gastrointestinal environment and intestinal epithelial

63 barriers have limited the use of oral vaccines. To interact with the abundant

64 immune cells in the lamina prima, an ideal oral vaccine must tolerate the

65 gastrointestinal environment and overcome intestinal epithelial barriers (23).

66 Exosomes are cell-derived, membranous vesicles present in nearly all bodily

67 fluids. With sizes ranging between 35-120 nm in diameter, exosomes are

68 composed of a phospholipid bilayer derived from the membrane of the cell of

69 origin. It has recently gained attention due to its natural role of shuttling

70 molecular cargos (e.g., DNA, small RNAs, proteins, and lipids) between distant

71 cells in the body. It has been confirmed that bovine milk is rich in exosomes and

72 exhibits the similar potential to serve as drug-delivery nanocarriers (24). Milk is a

73 more affordable and accessible source compared to cell culture media.

74 Moreover, milk-exos may provide additional benefits as naturally desirable oral

75 delivery carriers, which indicates that milk-exos constitute a more convenient

76 and patient-friendly therapeutic modality (25). Taking into account the biological

77 properties of milk exosomes and overcoming the technological challenges of

78 mRNA vaccines, we have currently described a method for creating milk

79 exosomes that are loaded with RBD mRNA, evaluated their effectiveness in

80 delivering functional mRNA, developed a novel oral vaccine technology platform

81 based on milk exosomes and investigated the preliminary efficacy of the novel

82 oral vaccine based on milk exosomes in mice to elicit humoral immunity to

83 SARS-CoV-2 spike proteins.

Results

Preparation of bovine milk-derived exosomes

86 To evaluate our preparation methods, bovine milk-derived exosomes (milk-exos)

87 were isolated and purified by density gradient ultracentrifugation (DC) (Fig. 1A).

88 Six components were collected by DC, among which F1 was about 5 mL, and F2

89 to F6 were all 7 mL (Fig. 1B). To characterize the isolated milk-exos

90 biophysically, biomarkers (CD9, TGS110), and morphology was used to

91 determine the exosomes containing fraction. Exosomes were mainly

92 concentrated in F3 and F4 (Fig. 1C, D). The morphology exhibited a rich

93 profusion of mixed populations of exosomes with predominantly intact vesicles

94 consistent with classical exosome-like morphology and a typical cup-like

95 structure (Fig. 1D). Milk exosomes are characteristic of exosomes in the range of

96 30-150 nm in diameter were observed in 0.95 mol/L-1.30 mol/L sucrose. As

97 fractions 3 and 4 were enriched in exosomes, they were pooled together for
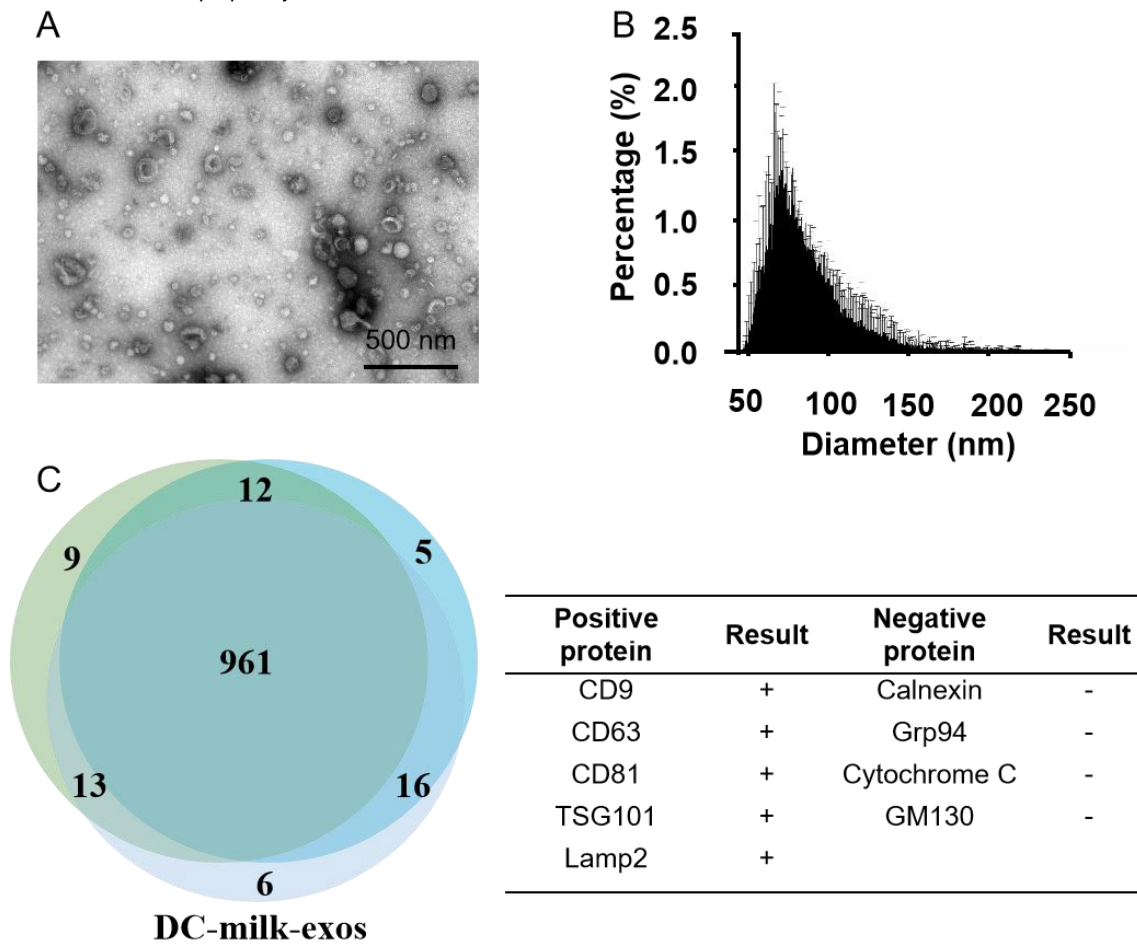
98 further analysis.
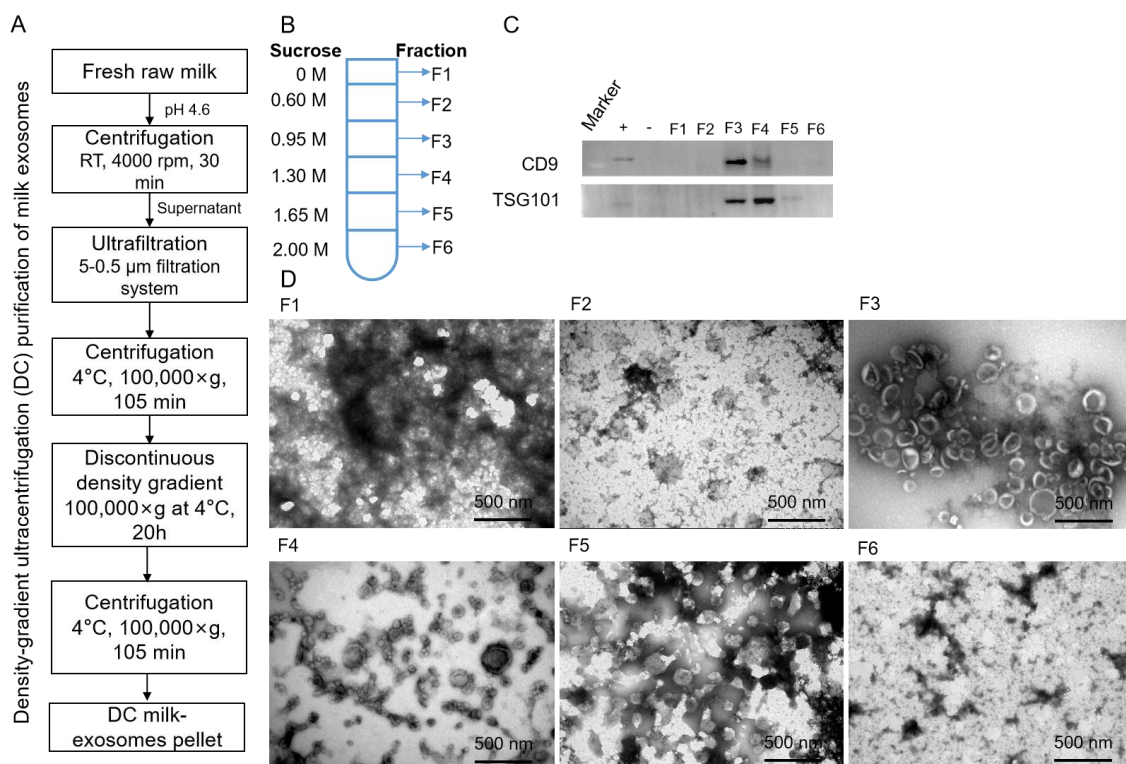
100 **Figure 1**. **Identification of bovine milk-derived exosomes in fractions of**

density gradient ultracentrifugation. (A) Schematic representation of the major steps involved in isolating of exosomes from bovine raw milk. (B) F1–F6 represents the corresponding concentrations of sucrose. (C) The exosome suspension was analyzed by western blot. Immunoblots showed exosomes marker in different milk exosome fractions. +, positive control (the protein of HaCat cells); -, negative control (the protein of Hela cells). (D) The morphology of different fractions obtained by TEM. (Scale bars = 500 nm).

Purification and characterization of bovine milk-derived exosomes by density gradient ultracentrifugation

The morphology of pooled exosomes fraction exhibited a rich profusion of exosomes consistent with classical exosome-like morphology (Fig. 2A), size distribution (Fig. 2B) and protein markers (Figure 2C). A three-way Venn diagram of proteins revealed 1022 proteins common to all datasets, and 961 proteins were commonly identified in all three DC-milk-exos, as shown in Figure 2C. Proteomics analysis of the samples showed that exosome protein lysates were prepared and verified with cluster analysis for vital exosomal membrane markers CD9, CD63, CD81, and TSG101. The absence of the microvesicle surface markers GM130 and calnexin, as well as the absence of the endoplasmic reticulum (ER) marker calnexin, confirmed that the isolated milk-exos were not contaminated with other multivesicular bodies (Fig. 2C). Three batches of bovine milk-derived exosomes obtained by density gradient ultracentrifugation (DC-milk-exos) were analyzed and indicated that there were no differences between multiple batches of DC-milk-exos.

Positive protein	Result	Negative protein	Result
CD9	+	Calnexin	-
CD63	+	Grp94	-
CD81	+	Cytochrome C	-
TSG101	+	GM130	-
Lamp2	+		

124

Figure 2. **Characterization of DC-milk-exos.** (A) The morphology and (B) the particle size analysis were detected by TEM and nanoFCM, respectively. (C) A three-way Venn diagram of proteins from three batches of DC-milk-exos revealed 1022 proteins common to all datasets. Cluster analysis for vital exosomal membrane markers CD9, CD63, CD81, TSG101, microvesicle surface markers GM130, and endoplasmic reticulum (ER) marker calnexin are indicated in the table. Abbreviations: TEM, transmission electron microscope; DC-milk-exos, bovine milk-derived exosomes by density gradient ultracentrifugation. Scale bars = 500 nm.

Loading of RBD mRNA Milk derived exosomes

To determine whether DC-milk-exos could be loaded with exogenous, *in vitro* synthesized mRNAs, we designed and synthesized a test receptor binding domain (RBD) mRNA encoding immunogenic forms of the SARS-CoV-2 spike. The RBD coding sequence region (CDS) is 675 base pairs (bp) long and has the

139 FLAG tag. Examination of the *in vitro* synthesized RBD mRNA using a

140 bioanalyzer (Agilent) confirmed that the RBD mRNA sample ran as a single band

141 of 1100 bps (Fig. 3A), consistent with the size that we expected to design in vitro

142 transcription. To assess its functionality, the RBD mRNA was transfected into

143 293T cells, and RBD peptide expression was interrogated the next day by

144 western blot (Fig. 3B). These results indicated that RBD mRNA was synthesized

145 according to in vitro transcription (IVT) and had a translational function that could

146 be translated into RBD protein in cells.

147
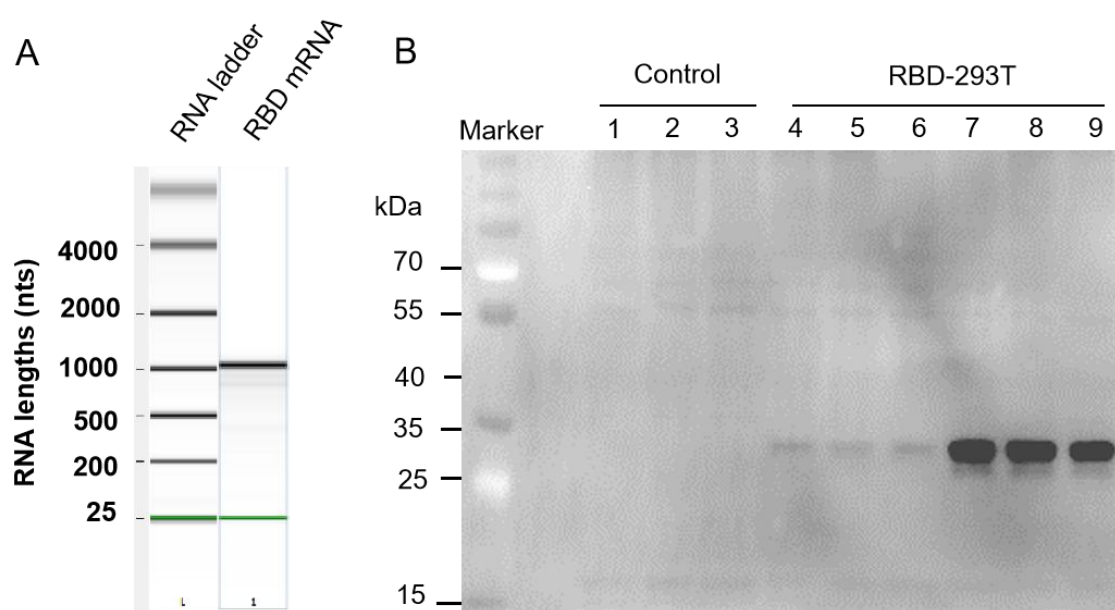
148 **Figure 3**. **Characterization of SARS-CoV-2 receptor binding domain (RBD)**

149 **mRNA.** (A) Gel-like image of in vitro synthesized RBD mRNA interrogated using

150 an RNA chip on an Agilent Bioanalyzer. Data for RNA markers, RBD mRNA, are

151 presented from left to right. (B) Western blot for SARS-CoV-2 RBD protein

152 expression in 293T cells when the RBD mRNA was transfected into 293T cells

153 with an additional 24 h of treatment along with 1 μg and 3 μg RBD mRNA. Lanes

154 1-3: control; Lanes 4-6: 1 μg RBD-293T; Lanes 7-9: 3 μg RBD-293T.

155 To load the IVT RBD mRNA into DC milk-exos, we first mixed it with cationic

156 lipids (DOTAP) to generate lipid mRNAs. Then we loaded the lipid-mRNA into

157 DC-milk-exos by mixing-induced partitioning (Fig. 4A). Both processes are

158 driven by the attractive force of the charge, resulting in the encapsulation of

159 lipid-mRNAs into Milk-exos membranes. To characterize the RBD mRNA

160 Milk-exos biophysically, the morphology and size distribution and zeta potential

161 analysis, were performed (Fig. 4B-D). To determine the loading efficiency of this

162 process, the products of three independent mRNA-loading reactions were

163 examined. A TaqMan-based real-time quantitative PCR assay showed that

164 loading efficiency reached 57.3% (Fig. 4E).

165
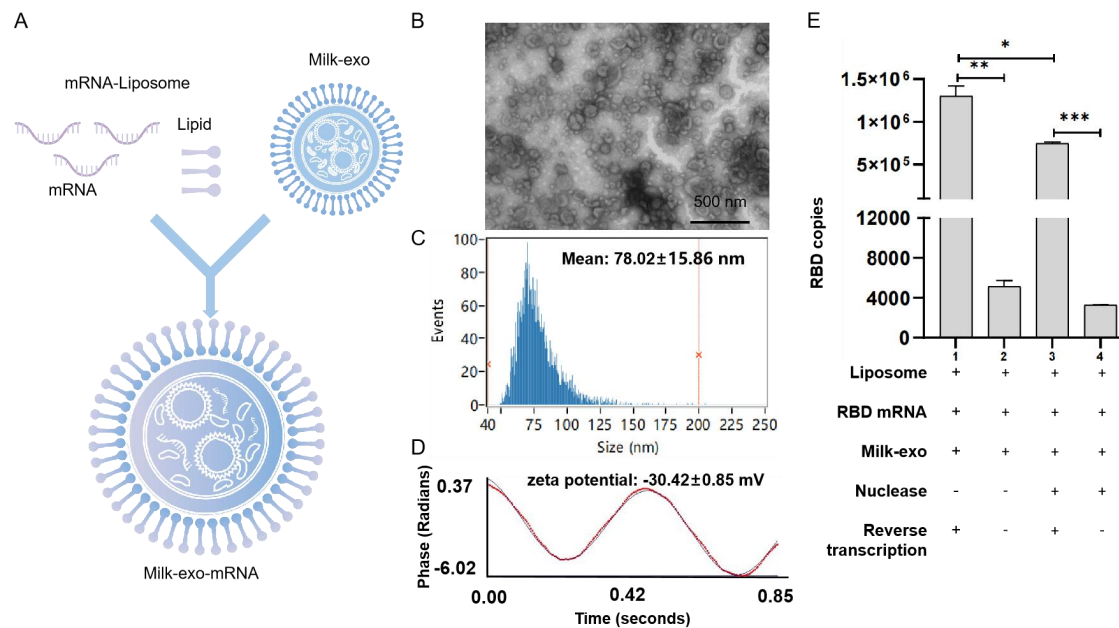
166 **Figure 4. Characterization of milk-derived exosome-based vaccine for**

167 **SARS-CoV-2.** (A) Flowchart of vaccine preparation for SARS-CoV-2. The

168 morphology (B), particle size distribution (C), zeta potential analysis (D), and

169 RBD mRNA loading efficiency (E) were executed. Scale bars = 500 nm.

170 **Verification of oral vaccines for RBD mRNA-DC-milk-exos *in vitro* and *in***

171 ***vivo***

172 We next tested whether Milk-exos loaded with RBD mRNA could deliver

173 functional RBD mRNA into human cells. Western blot and ELISA results

174 established that RBD mRNA-loaded Milk-exos could deliver mRNA into 293 cells

175 and produce RBD peptide 24 hr later.   (Fig. 5A, B, p<0.01).

176 To further confirm the ability to stimulate neutralizing antibodies, RBD

177 mRNA-milk-exos were injected into the duodenum (i. d.) of 9-11-week-old

178   female BALB/c mice (Fig. 6A). Blood (0.1 mL) was collected on days 0, 7, 14, 21,

179   28, 35, 42, and 49 for antibody detection before the animals were sacrificed.

180   Using ELISA kits adapted for detecting mouse-derived antibodies, we observed

181   that vaccinated animals produced a relatively constant level of neutralizing

182   antibodies against RBD after the second injection (Fig. 6B, C).

183
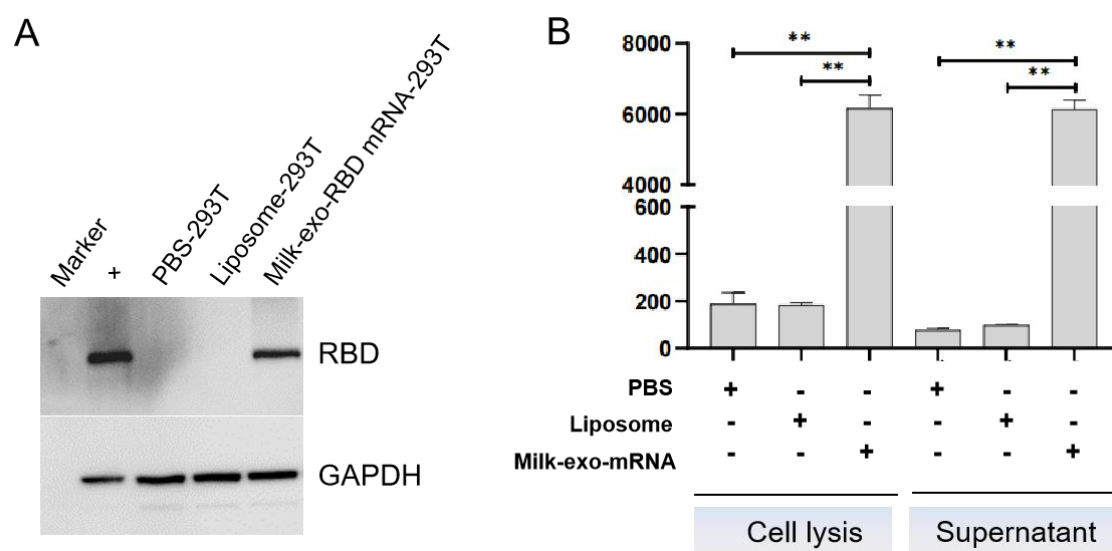
184   **Figure 5. mRNA-loaded exosomes deliver functional SARS-CoV-2 RBD**

185   **mRNA to human cells *in vitro*.**

186   (A) Western blot analysis of the expression of RBD mRNA delivered by oral

187   vaccine in 293T cells. (B) The ELISA detection of RBD expressed in 293T cell

188   lysate and secreted into the culture supernatant at 24 h after the milk-derived

189   exosome-based vaccine transfection. The data are presented as mean standard

190   deviation with a group size of three. **$P < 0.01$ vs. PBS.

191
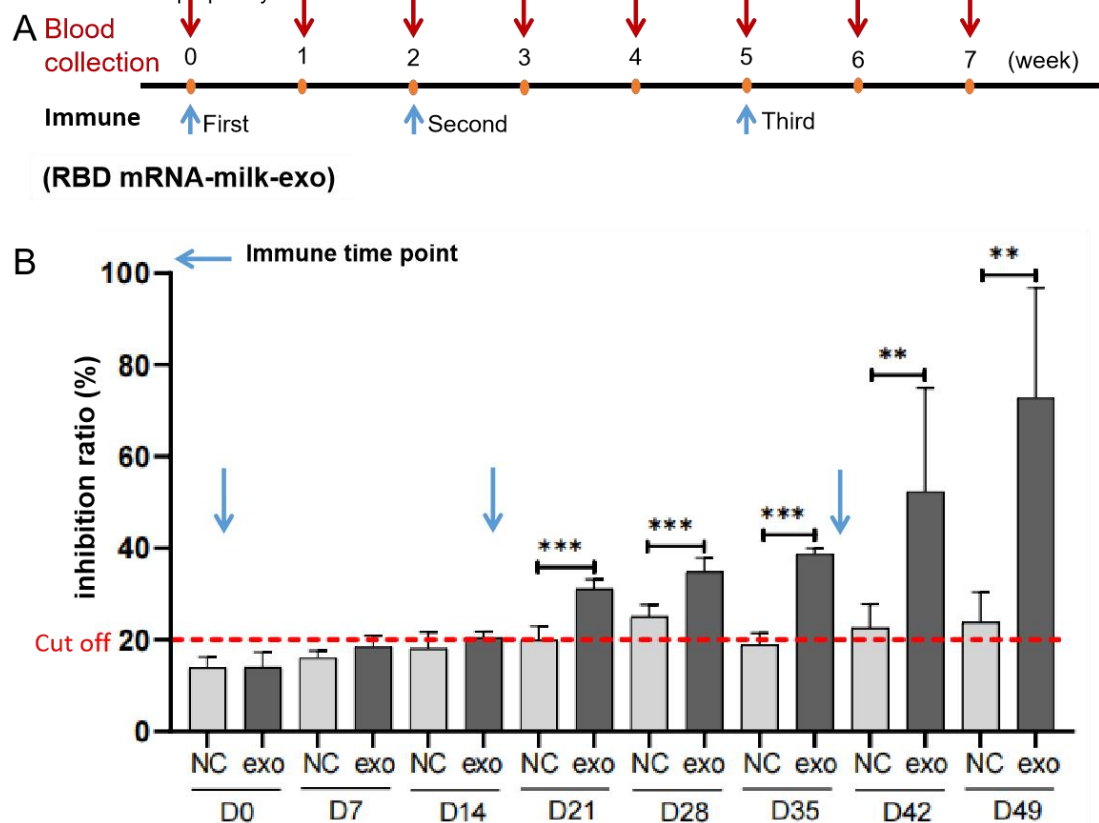
Figure 6. Validation of SARS-CoV-2 RBD mRNA-loaded milk exosomes delivering functional SARS-CoV-2 RBD mRNA *in vivo*.

(A) Mouse immunization and sera sampling schedule. BALB/c mice received the same doses of an oral vaccine for the SARS-CoV-2-based milk-derived exosomes (N = 5) or the control saline (N = 3) on day 0 and were boosted again on days 14 and 35. Sera were collected on days 0 (pre-vaccination), 7, 14, 21, 28, 35, 42 and 49 (post-vaccination). The blue and red arrow represented the time points of immunization and blood collection, respectively. (B) The neutralizing antibodies of the oral vaccine for SARS-CoV-2-based milk-derived exosomes in serum were determined by ELISA. The red dotted line represented the cutoff value of neutralizing antibodies against the RBD peptide. N = 3 (control), N = 5 (RBD-DC-milk-exos), and the data are presented as mean $\pm$ STD. **$P < 0.01$, ***$P < 0.001$ vs. control group.

Discussion

In this study, we demonstrated that an oral vaccine for SARS-CoV-2-based

207 bovine milk-derived exosomes could deliver functional mRNA *in vitro* and *in vivo*

208 and induce anti-S antibody responses. We first successfully verified the

209 technical feasibility of oral mRNA delivery based on bovine milk-derived

210 exosomes as delivery vehicles.

211 Compared with injection, oral administration was generally considered to have a

212 better safety profile, better patient compliance, and lower medical costs (20, 22).

213 Like liposomes, exosomes have a bi-lipid membrane and an aqueous core;

214 therefore, they could potentially be loaded with hydrophilic and lipophilic drugs

215 (26). However, the practical application of exosome-based therapeutics in

216 clinical transformation remained an ongoing challenge. Many studies isolated

217 exosomes from cell culture media with a low yield and cost, making scaling-up

218 production difficult (27). A cost-effective and scalable source should be optimized

219 based on the current limitations.

220 It was reported that bovine milk-derived exosomes exhibited a similar potential

221 to serve as drug-delivery nanocarriers (24). Milk was a more affordable and

222 accessible source compared to cell culture media. Moreover, bovine

223 milk-derived exosomes might provide additional benefits as naturally desirable

224 oral delivery carriers, which indicates that bovine milk-derived exosomes

225 constitute a more convenient and patient-friendly therapeutic modality (25).

226 Herein, we presented an oral vaccine that differed from previous

227 nanomaterials-based oral vaccine delivery technologies in that it comprised

228 bovine milk-derived exosomes, and the milk-derived exosome-derived oral

229 COVID-19 mRNA vaccine had its delivery technology and industrialization

230 capability. Although the results from this study suggested the beneficial effects of

231 an oral vaccine for the prevention of the novel coronavirus and offered a

232   potential regimen for clinical application, we needed to expand the number of

233   animals and further verify the efficacy of the oral vaccine in different animal

234   models (such as large animals) in future studies. Furthermore, the precise

235   molecular mechanisms and safety needed to be investigated further.

236   Although density-gradient ultracentrifugation has been the gold standard for

237   exosome isolation and purification, there have been several studies on the

238   extraction of exosomes from cow's milk using differential centrifugation alone (28,

239   29) or precipitation (30, 31) techniques. In conjunction with differential

240   centrifugation, we employed the density-gradient ultracentrifugation methods to

241   isolate exosomes from milk that were essentially free of contamination from

242   microvesicles. The final sample purity could reach 100%. In contrast, the

243   technique used in this study to purify exosomes is incompatible with large-scale

244   exosome production, which is one of the obstacles to the progress of

245   industrialization. The good news is that we have established the

246   chromatography-based novel manufacturing process to purify exosomes from

247   bovine milk with better quality than production by DC (data are not shown).

248   It will come soon that an mRNA delivery system based on milk-derived

249   exosomes will serve as a platform for mRNA therapeutics development in the

250   recent future.

251   **Materials and methods**

252   **Cell lines and cell culture**

253   293T cells (SCSP-502) (human embryonic kidney epithelial cells) were

254   purchased from the Cell Bank of the Typical Culture Preservation Committee,

255   Chinese Academy of Sciences (Shanghai, China). 293T cells were grown in

256   DMEM supplemented with 10% fetal bovine serum (FBS) and 1% penicillin/strep

257 solution at 37 °C and 5% CO_2 concentration in a humidified atmosphere. The

258 pooled cells were maintained in DMEM containing 10% (vol/vol) FBS, changing

259 the medium every other day. When the confluence of cultured cells reached 80%,

260 they were detached by treatment with 0.25% (wt/vol) trypsin and 0.1% (wt/vol)

261 ethylenediaminetetraacetic acid (Gibco) and reseeded at a density of 1×10^4 cells

262 per cm^2. Cultured cells before passage two were used for experiments. For RBD

263 mRNA expression *in vitro*, cells were transfected with mRNA using

264 Lipofectamine Messenger MAX, as suggested by the manufacturer (Thermo

265 Fisher).

266 **Density-gradient ultracentrifugation purification of milk-exos (The**

267 **DC-milk-exos)**

268 Milk exosomes were isolated by density-gradient ultracentrifugation (DC). Briefly,

269 the casein-free whey was centrifuged at 100,000 g (Beckman Coulter, USA) for

270 105 min to precipitate the milk-exos, resuspended in 1 mL PBS. The

271 concentrated milk-exos were subjected to the top of a discontinuous density

272 gradient consisting of 2 mol/L, 1.65 mol/L, 1.3 mol/L, 0.95 mol/L, and 0.6 mol/L

273 sucrose (7 mL volume for each angle) in 250 mM Tris-HCl solution (pH 7.4).

274 They were centrifuged at 100,000 g at 4 °C for 20h. The milk-exos fraction

275 between fractions 3 (1.3 mol/L) and 4 (1.65 mol/L) was collected. To remove

276 sucrose, the fraction was diluted in PBS to a final volume of 40 mL and

277 centrifuged at 100,000 g at 4 °C for 105 min. The pellet was resuspended in 1

278 mL of PBS. The DC-milk-exos were stored at -80 °C before use.

279 **Characterization of the DC-milk-exos morphology by transmission**

280 **electron microscopy**

281 The DC-milk-exos morphology was studied by transmission electron microscopy

282 (TEM), as described before, with some modifications. First, the DC-milk-exos

283 (100 µg/mL) were fixed by mixing with an equal volume of 4% (w/v)

284 paraformaldehyde at room temperature for 15 minutes. The selected sample (10

285 µL) was then subjected to a formvar-carbon-coated TEM grid and kept at room

286 temperature for 3 minutes. The grid was stained by adding 10 µL of uranyl

287 oxalate solution (4% uranyl acetate, 0.0075 M oxalic acids, pH 7). The stained

288 grid was investigated by a Hitachi 5600 plus transmission electron microscope

289 operated at 120 KV and 50,000 magnification.

290 **Measurement of the particle size distribution of DC-milk-exos by NanoFCM**

291 The particle size and number of milk-exos samples were characterized by the

292 NanoFCM instrument (NanoFCM Inc., Xiamen, China) by following the

293 operations manual. A silica nanosphere cocktail (Cat. S16M-Exo, NanoFCM Inc.,

294 Xiamen, China) containing a mixture of 68 nm, 91 nm, 113 nm, and 155 nm

295 standard beads was used to adjust the instrument for particle size measurement.

296 The instrumental parameters were set as follows: Laser, 10 mW, 488 nm; SS

297 decay, 10%; sampling pressure, 1.0 kPa; sampling period, 100 µs; time to record,

298 1 min.

299 **Proteomics**

300 The proteomics of DC-milk-exos was analyzed by LC–MS/MS using Easy

301 NLC1200-Q Exactive and Fusion Lumos Orbitrap mass spectrometers

302 (ThermoFisher), both fitted with nanoflow reversed-phase HPLC (Ultimate 3000

303 RSLC, Dionex). The nano-HPLC system was equipped with an Acclaim PepMap

304 nano-trap column (Dionex-C18, 100 Å, 75 µm × 2 cm) and an Acclaim Pepmap

305 RSLC analytical column (Dionex-C18, 100 Å, 75 µm × 25 cm). Typically, for

306 each LC-MS/MS experiment, 1 µL of the peptide mix was loaded onto the

307 enrichment (trap) column at an isocratic flow of 5 µL/min of 3% CH3CN

308 containing 0.1% formic acid for 5 min before the enrichment column was

309 switched in-line with the analytical column. The eluents used for the LC were

310 0.1% (v/v) formic acid (solvent A) and 100% CH3CN/0.1% (v/v) formic acid. The

311 gradient used was 3% B to 25% B for 23 min, 25% B to 40% B in 2 min, 40% B

312 to 85% B in 2 min, and maintained at 85% B for 2 min before equilibration for 10

313 min at 3% B before the next injection. All spectra were collected in positive mode

314 using full-scan MS spectra scanning in the FT mode from m/z 300-1650 at

315 resolutions of 70 000 (QE) and 120,000 (Lumos). A lock mass of 445.12003 m/z

316 was used for both instruments. For MS/MS on the Lumos, the "top speed"

317 acquisition mode (3 s cycle time) on the most intense precursor was used,

318 whereby peptide ions with charge states ≥2 were isolated with an isolation

319 window of 1.6 m/z and fragmented with HCD using a normalized collision energy

320 of 35. For MSMS on the QE plus, the 15 most intense peptide ions with charge

321 states ≥2 were isolated with an isolation window of 1.6 m/z and fragmented by

322 HCD with a normalized collision energy of 35. A dynamic exclusion of 30

323 seconds was applied.

324 The raw files were searched using Proteome Discover (version 2.1, Thermo

325 Fisher, Germany) with Sequest as the search engine. Fragment and peptide

326 mass tolerances were set at 20 mDa and 10 ppm, respectively, allowing a

327 maximum of 2 missed cleavage sites. The false discovery rates of proteins,

328 peptides, and phosphosites were 1 percent. The differential expression proteins

329 were analyzed by DAVID (Database for Annotation, Visualization, and

330 Integrated Discovery) Bioinformatics Resource 2021

331 (http://david.abcc.ncifcrf.gov/) with recommended analytical parameters to

332 identify the most significantly enriched signal transduction pathways in the data

333 set.

334 **Western blot**

335 Total cellular and milk-exos proteins were extracted with RIPA lysis buffer, and

336 the protein concentration was determined by a BCA protein assay kit (Thermo,

337 A53226). Following that, the protein was loaded onto SDS-polyacrylamide gel

338 electrophoresis gels. After electrophoresis, proteins were transferred onto a

339 polyvinylidene fluoride membrane and blocked in 5% (wt/vol) bovine serum

340 albumin (BSA) for 1 hour at room temperature. Then the membrane was

341 incubated with anti-TSG101 (Abcam, ab125011), anti-CD9 (Abcam, ab92726),

342 anti-RBD (Abcam, ab277628), or anti-GAPDH (Proteintech, 60004-1) overnight

343 at 4 °C. After washing in Tris-buffered saline with Tween (TBST), the

344 horseradish peroxidase (HRP) secondary antibody was diluted 1:10,000 with 5%

345 (wt/vol) BSA and incubated with the membrane for 1 hour at room temperature.

346 Excess secondary antibody was rinsed off the membrane with TBST, and a

347 chemiluminescent signal was generated using the FluorChem E system

348 (ProteinSimple, USA) according to the manufacturer's protocol.

349 **Measurement of zeta potential**

350 The Zeta potential of milk exosomes was measured thrice at 25 °C under the

351 following settings: sensitivity of 85, a shutter value of 70, and a frame rate of 30

352 frames per second, while ZetaView software was used to collect and analyze the

353 data.

354 **Construction of an oral vaccine for SARS-CoV-2 RBD-based**

355 **DC-milk-derived exosomes (RBD-DC-milk-exos)**

356 mRNA designed to express the RBD proteins was obtained from a commercial

357 provider (Novoprotein). RBD mRNAs were purified using CIMmultus Oligo dT

358 columns and resuspended in DNase- and RNase-free water using nuclease-free

359 tips and tubes. Purified RBD mRNAs were prepared for loading into

360 DC-milk-exos by preincubating them with cationic lipids, generating a

361 lipid-mRNA product. Lipid-mRNAs were subsequently loaded into purified DC-

362 milk-exos by mixing and incubation to construct an oral vaccine. The

363 morphology, particle size distribution, and zeta potential of RBD mRNA-loaded

364 DC-milk-exos were characterized by TEM, the NanoFCM instrument, and Zeta

365 Pals, respectively. RBD mRNA loading efficiency was detected by

366 Taqman-based quantitative real-time PCR (qRT-PCR). RBD mRNA expression

367 was measured using western blot and enzyme-linked immunosorbent assay

368 (ELISA).

RNA extraction and Taqman-based RT-qPCR assay

370 Total RNA was extracted from the RBD-DC-milk-exos using TRIzol (Life

371 Technologies, Carlsbad, CA). First-strand cDNA was synthesized using the

372 PrimeScript^{TM} RT Kit (TaKaRa, Beijing, China) and used as a template to

373 determine the expression of RBD genes with the indicated primers and probes.

374 The following primer sequences were used: RBD, forward 5'-CTCCAGGGCAA

375 ACTGGAAAG-3', and reverse 5'-AATTACCACCAACCTTAGAATCAAG-3',

376 probe, CCAGATGATTTTACAGGCTGCGTTATAG, using Premix Ex Taq™

377 (Probe qPCR) reagent (TaKaRa, Beijing, China) in qRT-PCR. The cycling

378 parameters were as follows: a PCR reaction was carried out on 50 ng of cDNA

379 samples using 0.2 µmol/L of each primer, 0.4 µmol/L RBD probe, and 10 µL

380 2×Premix Ex Taq Mix. The following conditions were used: 95 °C for 30 s, 40

381 cycles at 95 °C for 5 s, and 60 °C for 31 s in a Thermofisher QuantStudio5 and

382 analyzed with the dedicated software.

ELISA assay

384 The cell lysate, culture supernatant, and serum were homogenized for protein

385 extraction. The spike protein RBD (Beyotime, Shanghai, China) and neutralizing

386 antibody (Vazyme, Nanjing, China) expressions were determined using ELISA

387 kits according to the manufacturer's instructions.

Measurement of RBD activity *in vitro*

389 We tested whether an oral vaccine for SARS-CoV-2 RBD-based

390 DC-milk-derived exosomes (RBD-DC-milk-exos) could deliver functional RBD

391 mRNA into human cells. For *in vitro* studies, the oral vaccine added the resulting

392 formulations to cultures of human cells, grew the cells overnight to allow for RBD

mRNA uptake and expression, and then assayed the cells for RBD activity by western blot and ELISA.

Delivery function verification of RBD-DC-milk-exos *in vivo*.

We used age-matched female BALB/c mice (Speford (Beijing) Biotechnology Co., Ltd.). All animal experimentation was performed following institutional guidelines for animal care and use and was approved by the Experimental Animal Ethics Committee of Youji (Tianjin) Pharmaceutical Technology Co., Ltd. (IACUC-20220726-05.00). Female BALB/c mice (23~26 g, Speford, Beijing, China) were housed in a pathogen-free facility with standard conditions of temperature 24 $^\circ$ C, a 12-hour light/dark cycle, and food and water ad libitum. Mice were employed to study the activity of RBD mRNA-DC-milk-exos administered via duodenal injection. Mice were randomly divided into 2 groups: 1) the control group (saline, 1000 µL) (N = 3); and 2) the RBD-DC-milk-exos (0.5 mg mRNA/1000 µL) group (N = 5). All treatments were started by duodenal injection on days 1, 15, and 36. All mice were sacrificed two weeks after the last treatmen with 1% isoflurane. Blood was collected at different time points (days 0, 7, 14, 21, 28, 35, 42, and 49). Verification of neutralizing antibodies of the oral vaccine for SARS-CoV-2-based milk-derived exosomes *in vivo* was executed by ELISA analysis in serum. N = 3 (control), N = 5 (RBD mRNA-DC-milk-exos), and the data are presented as mean $\pm$ STD. **P < 0.01, ***P < 0.001 vs. control group.

Statistical analyses

The data were represented as the mean and standard deviation. An unpaired student's t-test was used to analyze data with only two sets. A one-way analysis of variance (ANOVA) was performed to determine whether there was a significant difference between more than two datasets, followed by Bonferroni's post hoc test using GraphPad Prism 6.0. P < 0.05 was considered statistically

420 significant for group differences. Asterisk (*) represented P < 0.05; a double

421 asterisk (**) represented P < 0.01; a triple asterisk (***) represented P < 0.001.

422 **References**

423 1. Yang X, Yu Y, Xu J, Shu H, Xia J, Liu H, et al. Clinical course and outcomes of

424 critically ill patients with SARS-CoV-2 pneumonia in Wuhan, China: a

425 single-centered, retrospective, observational study. Lancet Respir Med (2020)

426 8(5): 475-481. doi: 10.1016/S2213-2600(20)30079-5

427 2. Lauer SA, Grantz KH, Bi Q, Jones FK, Zheng Q, Meredith HR, et al. The

428 Incubation Period of Coronavirus Disease 2019 (COVID-19) From Publicly

429 Reported Confirmed Cases: Estimation and Application. *Ann Intern Med* (2020)

430 172(9): 577-582. doi: 10.7326/M20-0504

431 3. Huang NE, Qiao F. A data driven time-dependent transmission rate for

432 tracking an epidemic: a case study of 2019-nCoV. *Sci Bull (Beijing)* (2020) 65(6):

433 425-427. doi: 10.1016/j.scib.2020.02.005

434 4. Zhou P, Yang XL, Wang XG, Hu B, Zhang L, Zhang W, et al. A pneumonia

435 outbreak associated with a new coronavirus of probable bat origin. *Nature* (2020)

436 579(7798):270-273. doi: 10.1038/s41586-020-2012-7

437 5. Walls AC, Park YJ, Tortorici MA, Wall A, McGuire AT, Veesler D. Structure,

438 Function, and Antigenicity of the SARS-CoV-2 Spike Glycoprotein. *Cell* (2020)

439 183(6):1735. doi: 10.1016/j.cell.2020.02.058

440 6. Letko M, Marzi A, Munster V. Functional assessment of cell entry and receptor

441 usage for SARS-CoV-2 and other lineage B betacoronaviruses. *Nat Microbiol*

442 (2020) 5(4):562-569. doi: 10.1038/s41564-020-0688-y

443 7. Hoffmann M, Kleine-Weber H, Schroeder S, Kruger N, Herrler T, Erichsen S,

444 et al. SARS-CoV-2 Cell Entry Depends on ACE2 and TMPRSS2 and Is Blocked

445 by a Clinically Proven Protease Inhibitor. *Cell* (2020) 181(2):271-280.e278. doi:

446 10.1016/j.cell.2020.02.052

447   8. Li W, Moore MJ, Vasilieva N, Sui J, Wong SK, Berne MA, et al.

448   Angiotensin-converting enzyme 2 is a functional receptor for the SARS

449   coronavirus. *Nature* (2003) 426(6965):450-454. doi: 10.1038/nature02145

450   9. Li F, Li W, Farzan M, Harrison SC. Structure of SARS coronavirus spike

451   receptor-binding domain complexed with receptor. *Science* (2005)

452   309(5742):1864-1868. doi: 10.1126/science.1116480

453   10. Andersen KG, Rambaut A, Lipkin WI, Holmes EC, Garry RF. The proximal

454   origin of SARS-CoV-2. *Nat Med* (2020) 26(4):450-452. doi:

455   10.1038/s41591-020-0820-9

456   11. Hossain MK, Hassanzadeganroudsari M, Feehan J, Apostolopoulos V. The

457   race for a COVID-19 vaccine: where are we up to? *Expert Rev Vaccines* (2022)

458   21(3):355-376. doi: 10.1080/14760584.2022.2021074

459   12. Polack FP, Thomas SJ, Kitchin N, Absalon J, Gurtman A, Lockhart S, et al.

460   Safety and efficacy of the BNT162b2 mRNA covid-19 vaccine. *New Engl J Med*

461   (2020) 383(27):2603-2615. doi: 10.1056/NEJMoa2034577

462   13. Ho W, Gao M, Li F, Li Z, Zhang XQ, Xu X. Next-generation vaccines:

463   Nanop-articl-mediated DNA and mRNA delivery. *Adv Healthc Mater* (2021)

464   10(8):e2001812. doi: 10.1002/adhm

465   14. Kariko K, Muramatsu H, Welsh FA, Ludwig J, Kato H, Akira S, et al.

466   Incorporation of pseudouridine into mRNA yields superior nonimmunogenic

467   vector with increased translational capacity and biological stability. *Mol Ther*

468   (2008) 16(11):1833-1840. doi: 10.1038/mt.2008.200

469   15. Thess A, Grund S, Mui BL, Hope MJ, Baumhof P, Fotin-Mleczek M, et al.

470   Sequence-engineered mRNA without chemical nucleoside modifications

471   enables an effective protein herapy in large animals. *Mol Ther* (2015)

472   23(9):1456-1464. doi: 10.1038/mt.2015.103

473   16. Kariko K, Muramatsu H, Ludwig J, Weissman D. Generating the optimal

474   mRNA for therapy: HPLC purification eliminates immune activation and improves

475   translation of nucleoside-modified, protein-encoding mRNA. *Nucleic Acids Res*

476   (2011) 39(21):e142. doi: 10.1093/nar/gkr695

477   17. Alberer M, Gnad-Vogt U, Hong HS, Mehr KT, Backert L, Finak G, et al. Safety

478   and immunogenicity of a mRNA rabies vaccine in healthy adults: An open-label,

479   non-randomised, prospective, first-in-human phase I clinicia trial. *Lancet* (2017)

480   390(10101):1511-1520. doi: 10.1016/S0140-6736(17)31665-3

481   18. Zhang Z, Mateus J, Coelho CH, Dan JM, Moderbacher CR, Galvez RI, et al.

482   Humoral and cellular immune memory to four COVID19 vaccines. *Cell.* (2022)

483   185(14):2434-2451. doi: 10.1016/j.cell.2022.05.022

484   19. Laczko D, Hogan MJ, Toulmin SA, Hicks P, Lederer K, Gaudette BT, et al. A

485   single immunization with nucleoside-modified mRNA vaccines elicits strong

486   cellular and humoral immune responses against SARS-CoV-2 in mice. *Immunity*

487   (2020) 53(4):724-732e7. doi: 10.1016/j.immuni.2020.07.019

488   20. Vela Ramirez JE, Sharpe LA, Peppas NA. Current state and challenges in

489   developing oral vaccines. *Adv Drug Deliv Rev* (2017) 114, 116–131. doi:

490   10.1016/j.addr.2017.04.008

491   21. Qin H, Zhao R, Qin Y, Zhu J, Chen L, Di C, et al. Development of a cancer

492   vaccine using in vivo click-chemistry-mediated active lymph node accumulation

493   for improved immunotherapy. *Adv Mater* (2021) 33(20): e2006007. doi:

494   10.1002/adma.202006007

495   22. Taddio A, Ipp M, Thivakaran S, Jamal A, Parikh C, Smart S, et al. Survey of

496   the prevalence of immunization non-compliance due to needle fears in children

497   and adults. *Vaccine* (2012) 30(32):4807–4812. doi:

498   10.1016/j.vaccine.2012.05.011

499   23. Kim SH, Jang YS. The development of mucosal vaccines for both mucosal

500   and systemic immune induction and the roles played by adjuvants. *Clin Exp*

Vaccine Res (2017) 6(1):15–21. doi: 10.7774/cevr.2017.6.1.15

24. Somiya M, Yoshioka Y, Ochiya T. Biocompatibility of highly purified bovine milk-derived extracellular vesicles. *J Extracell Vesicles* (2018) 7(1):1440132. 10.1080/20013078.2018.1440132

25. Li D, Yao S, Zhou Z, Shi J, Huang Z, Wu Z. Hyaluronan decoration of milk exosomes directs tumor-specific delivery of doxorubicin. *Carbohydr Res* (2020) 493:108032. 10.1016/j.carres.2020.108032

26. Vlassov AV, Magdaleno S, Setterquist R, Conrad R. Exosomes: current knowledge of their composition, biological functions, and diagnostic and therapeutic potentials. *Biochim Biophys Acta* (2012) 1820(7):940-948. doi: 10.1016/j.bbagen.2012.03.017

27. Aqil F, Munagala R, Jeyabalan J, Agrawal AK, Kyakulaga AH, Wilcher SA, et al. Milk exosomes-natural nanoparticles for siRNA delivery. *Cancer Lett* (2019) 449:186-195. 10.1016/j.canlet.2019.02.011

28. Wolf T, Baier SR, Zempleni J. The intestinal transport of bovine milk exosomes is mediated by endocytosis in human colon carcinoma Caco-2 cells and rat small intestinal IEC-6 cells. *J Nutr* (2015) 145(10):2201–2206. doi: 10.3945/jn.115.218586

29. Izumi H, Tsuda M, Sato Y, Kosaka N, Ochiya T, Iwamoto H, et al., Bovine milk exosomes contain microRNA and mRNA and are taken up by human macrophages. *J Dairy Sci* (2015) 98(5):2920–2933. doi: 10.3168/jds.2014-9076

30. Pieters BC, Arntz OJ, Bennink MB, Broeren MG, van Caam AP, Koenders MI, et al. Commercial cow milk contains physically stable extracellular vesicles expressing immunoregulatory TGF-beta. *PLoS ONE* (2015) 10(3):e0121123. doi: 10.1371/journal.pone.0121123

526   31. Yamada T, Inoshima Y, Matsuda T, Ishiguro N. Comparison of methods for

527   isolating exosomes from bovine milk. *J Vet Med Sci* (2012) 74(11):1523–1525.

528   doi: 10.1292/jvms.12-0032

535   **Author contributions:** All authors reviewed the manuscript; X.H.G., L.L., Q.Z.,

536   M.W., and C.L.H. formulated ideas, designed the study and experiments. Q.Z.,

537   M.W., C.L.H., and Z.J.W. performed experiments and produced reagents; L.L,

538   Q.Z., M.W., C.L.H., X.Z.M., D.L.Q., N.W., and J.H.W. analyzed experimental

539   data; H.Q.D. supervised work. L.L. and Q.Z. wrote the manuscript. All authors

540   contributed to the article and approved the submitted version.

541   **Conflict of interest:** The authors declare that the research was conducted in

542   the absence of any commercial or financial relationships that could be construed

543   as a potential conflict of interest.

544   **Data and materials availability:** All data are available in the main text or the

545   supplementary materials. Further inquiries can be directed to the corresponding

546   author.

547   **Ethics statement:** The animal study was reviewed and approved by the

548   Experimental Animal Ethics Committee of Youji (Tianjin) Pharmaceutical

549   Technology Co., Ltd. (IACUC-20220726-05.00).